Supporting Information

Impact of side-chain deuteration on the molecular stacking and photovoltaic performance of non-fullerene acceptors

Liang Zeng,[a] Ming Zhang,[a] Mengyuan Gao[b], Lingwei Xue [c], Haiqiao Wang [d], Zhi-Guo Zhang*[a], Long Ye*[b],

[a] State Key Laboratory of Chemical Resource Engineering, Beijing Advanced Innovation Center for Soft Matter Science and Engineering, Beijing University of Chemical Technology, Beijing 100029, China.

[b] School of Materials Science and Engineering, Tianjin Key Laboratory of Molecular Optoelectronic Sciences, Tianjin University, Collaborative Innovation Center of Chemical Science and Engineering (Tianjin), Tianjin, China..

[c] School of Chemical and Environmental Engineering, Pingdingshan University, Pingdingshan Henan 467000, China

[d] Beijing Engineering Research Center for the Synthesis and Applications of Waterborne Polymers, Beijing University of Chemical Technology, Beijing 100029, China

Email addresses: yelong@tju.edu.cn; zgzhangwhu@iccas.ac.cn

Contents

1.Materials and Synthesis

Materials: All the other chemicals were purchased as reagent grade from J&K, Macklin, and Bidepharm, and used without further purification. All solvents for reactions were accessed through commercial channels and distilled immediately prior to use.

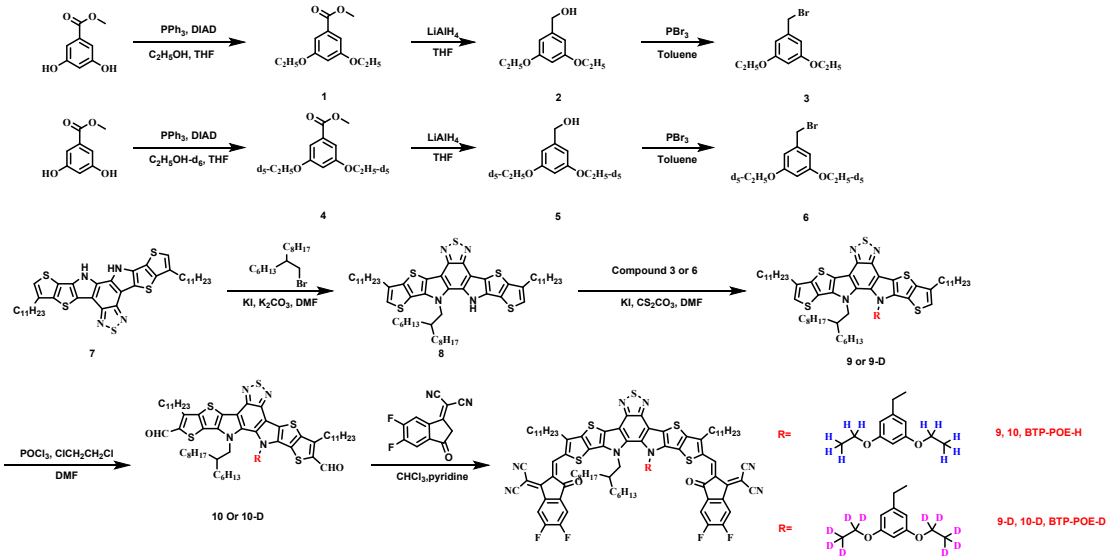

Scheme S1. The synthetic routes of BTP-POE-H and BTP-POE-D

Compound 1: methyl 3,5-dihydroxybenzoate (2.52 g, 1.50 mmol), triphenylphosphine (9.83 g, 3.75 mmol) anhydrous THF (60 mL) were added sequentially to a 250 mL two-necked round-bottom flask. After displacing argon gas three times and the reaction was cooled to 0 °C in an ice bath. Ethanol (1.72 g, 3.75 mmol) was added to the reaction followed by slow addition of DIAD (7.57 g, 3.75 mmol) and stirred at 0 °C for 1 h. The reaction was then removed from the ice bath and heated to reflux for 18 h. The reaction mixture was then cooled to room temperature and then extracted with dichloromethane. The organic layer was washed with brine and dried over $MgSO_4$. After filtration, the crude product was purified by

flash column chromatography with petroleum ether (PE) and dichloromethane (DCM) (2:1) as the eluents to afford the final product as a white solid. (2.78 g, 82.6%). ^{1}H NMR (400 MHz, $CDCl_3$) δ 7.16 (d, *J* = 2.3 Hz, 2H), 6.63 (t, *J* = 2.2 Hz, 1H), 4.05 (q, *J* = 7.0 Hz, 4H), 3.89 (s, 3H), 1.41 (t, *J* = 7.0 Hz, 7H).

Compound 2:Compound 1 (2.78 g, 1.24 mmol) and 40 ml of TFH were added to a 100 mL double-necked round-bottom flask and the reaction was brought to 0°C in an ice-cold bath. $LiAlH_4$ (94 mg, 2.48 mmol) was then slowly added and stirred at low temperature for 4 h. The reaction was quenched with water and extracted with DCM. The organic layer was washed with brine and dried over $MgSO_4$. After filtration, the crude product was purified by flash column chromatography with petroleum ether and Ethyl acetate (4:1) as the eluents to afford the final product as a white solid (2.25 g, 92.4%). ^{1}H NMR (400 MHz, $CDCl_3$) δ 6.52 (s, 2H), 6.38 (s, 1H), 5.30 (s, 1H), 4.65 (s, 2H), 4.04 (q, *J* = 7.0 Hz, 4H), 1.43 (t, *J* = 7.0 Hz, 6H).

Compound 3:The compound 2 (2.25 g, 1.16 mmol) was dissolved in toluene (50 ml), the solution was cooled down by ice water bath. PBr_3 (0.43 ml, 28 mmol) was added to the solution. The mixture was stirred at room temperature for 12 h under argon. Ice water (20 ml) was added to the mixture to eliminate PBr_3, then the mixture was extracted by DCM. The organic layer was washed with brine and dried over $MgSO_4$. After filtration, the crude product was purified by flash column chromatography with PE:DCM =2:1 as the eluents to afford the final product as a white solid (2.18 g, 72.6%). ^{1}H NMR (400 MHz, $CDCl_3$) δ 6.51 (d, *J* = 2.1 Hz, 2H), 6.37 (t, *J* = 2.0 Hz, 1H), 4.40 (s, 2H), 4.01 (q, *J* = 7.0 Hz, 5H), 1.40 (t, *J* = 6.0 Hz, 7H).

Compound 4: According to the synthetic process of compound **1**, and using ethanol-d_6 (1 g, 1.92 mmol) instead of Ethanol, compound **4** was obtained as white solid (1.45 g, 81.2%) . ^{1}H NMR (400 MHz, $CDCl_3$) δ 7.16 (d, *J* = 2.3 Hz, 2H), 6.63 (t, *J* = 2.3 Hz, 1H), 3.89 (s, 3H).

Compound 5: According to the synthetic process of compound **2**, and using Compound **4** (1.45 g, 6.19 mmol) instead of Compound **1**, compound **5** was obtained as white solid (1.12 g, 92.6%) . ^{1}H NMR (400 MHz, $CDCl_3$) δ 6.49 (d, *J* = 2.0 Hz, 2H), 6.36 (t, *J* = 2.1 Hz, 1H), 4.60 (s, 2H), 1.82 (s, 1H).

Compound 6: According to the synthetic process of compound **3**, and using Compound **5** (1.12 g, 5.43 mmol) instead of compound **2** , compound **6** was obtained as white solid (1.00 g, 68.9%).^{1}H NMR (400 MHz, $CDCl_3$) δ 6.51 (d, *J* = 2.2 Hz, 2H), 6.37 (t, *J* = 2.2 Hz, 1H), 4.40 (s, 2H).

Compound 8: To a 50 mL two-necked round bottom flask, compound **7** (747 mg, 1 mmol), 7-(bromomethyl)pentadecane (305 mg, 1 mmol), K_2CO_3 (165 mg, 1.2 mmol), KI (16.6 mg, 0.2 mmol) and DMF (20 mL) were added. After displacing argon gas three times and the mixture was stirred at 80 °C for 12 h and then cooled down to room temperature. Brine was added and the mixture was extracted with dichloromethane. The organic phase was dried over anhydrous $MgSO_4$ and filtered. After removing the solvent from the filtrate, the residue was purified by column chromatography on silica gel using PE:DCM (3:1) as the eluent yielding a red solid (610 mg, 62.8%). ^{1}H NMR (400 MHz, $CDCl_3$) δ 8.36 (s, 1H), 6.89 (s, 2H), 4.03 (s,

2H), 2.68 (s, 4H), 1.93 (s, 1H), 1.81 (s, 4H), 1.52 - 1.10 (m, 56H), 0.93 - 0.74 (m, 12H).

Compound 9: To a 50 mL two-necked round bottom flask, compound **8** (305 mg, 0.314 mmol), Compound **3** (330 mg, 1.33 mmol), K_2CO_3 (86 mg, 0.628 mmol), KI (10 mg, 0.063 mmol) and DMF (20 mL) were added. After displacing argon gas three times and the mixture was stirred at 80 °C for 12 h and then cooled down to room temperature. Brine (30 mL) was added and the mixture was extracted with DCM. The organic phase was dried over anhydrous $MgSO_4$ and filtered. After removing the solvent from the filtrate, the residue was purified by column chromatography on silica gel using PE:DCM (3:1) as the eluent yielding an orange solid (266 mg, 73.6%).^{1}H NMR (400 MHz, $CDCl_3$) δ 6.95 (s, 1H), 6.81 (s, 1H), 6.65 (d, *J* = 1.6 Hz, 2H), 6.46 (s, 1H), 5.57 (s, 2H), 4.26 (d, *J* = 7.8 Hz, 2H), 3.97 (q, *J* = 6.9 Hz, 4H), 2.76 (t, *J* = 7.7 Hz, 2H), 2.69 (t, *J* = 7.6 Hz, 2H), 2.02 - 1.92 (m, 1H), 1.80 (m, 4H), 1.47 - 0.43 (m, 74H).

Compound 9-D: According to the synthetic process of compound **9**, and using Compound **6** (338 mg, 1.33 mmol) instead of Compound **3** , compound **9** was obtained as orange solid(263 mg, 72.3%).^{1}H NMR (400 MHz, $CDCl_3$) δ 6.95 (s, 1H), 6.82 (s, 1H), 6.65 (d, *J* = 1.9 Hz, 2H), 6.46 (t, *J* = 2.0 Hz, 1H), 5.58 (s, 2H), 4.26 (d, *J* = 7.8 Hz, 2H), 2.76 (t, *J* = 7.7 Hz, 2H), 2.69 (t, *J* = 7.7 Hz, 2H), 2.03 - 1.92 (m, 1H), 1.80 (m, 4H), 1.48 - 0.42 (m, 68H).

Compound 10: To a 25 mL two-necked round bottom flask were added $POCl_3$ (0.5 mL) and DMF (2.5 mL) under the protection of nitrogen and the solution was stirred

at 0 °C for 2 h. Then, compound 9 (115 mg, 0.1 mmol) in 1,2-dichloroethane solution(10 mL) was added. After stirring at 80 C for 12 h, the mixture was quenched with saturated $NaHCO_3$ (aq) and extracted with DCM. The organic phase was dried over anhydrous $MgSO_4$ and filtered. After removing the solvent from the filtrate, the residue was purified by column chromatography on silica gel using PE:DCM (2:1) as the eluent yielding an orange solid (102 mg, 84.6%).^{1}H NMR (400 MHz, $CDCl_3$) δ 10.10 (s, 1H), 10.03 (s, 1H), 6.60 (d, *J* = 1.7 Hz, 2H), 6.47 (s, 1H), 5.67 (s, 2H), 4.33 (d, *J* = 7.8 Hz, 2H), 4.00 (q, *J* = 6.9 Hz, 4H), 3.23 - 3.07 (m, 4H), 2.00 - 1.82 (m, 5H), 1.49 - 0.41 (m, 74H).

Compound 10-D: According to the synthetic process of compound **10**, and using Compound **9-D** (116 g, 0.1 mmol) instead of Compound **9**, compound **10-D** was obtained as orange solid (99 mg, 81.6%).^{1}H NMR (400 MHz, $CDCl_3$) δ 10.09 (s, 1H), 10.02 (s, 1H), 6.59 (d, *J* = 1.7 Hz, 2H), 6.47 (s, 1H), 5.68 (s, 2H), 4.30 (d, *J* = 7.8 Hz, 2H), 3.12 (m, 4H), 2.00 - 1.82 (m, 5H), 1.49 - 0.40 (m, 68H).

BTP-POE-H: To a 50 mL three-necked round bottom flask, compound 10 (102 mg, 0.085 mmol), 2-(5,6-difluoro-3-oxo-2,3-dihydro-1H-inden-1-ylidene)malononitrile (78 mg, 0.34 mmol), 20 mL chloroform and 0.5 mL pyridine. After displacing argon gas three times and then stirring at reflux for 12 h. Allow the reaction solution to cool to room temperature, pour it into methanol (150 ml) and filter. the residue was purified by column chromatography on silica gel using PE:DCM (1:1) as the eluent yielding a blue-black solid (109 mg,78.9%).^{1}H NMR (400 MHz, $CDCl_3$) δ 8.82 (s, 1H), 8.51 (dd, *J* = 9.9, 6.5 Hz, 1H), 8.35 (dd, *J* = 9.8, 6.8 Hz, 2H), 7.58 (t, *J* = 7.5 Hz,

1H), 7.42 (t, *J* = 7.5 Hz, 1H), 6.72 (s, 2H), 6.53 (s, 1H), 5.91 (s, 2H), 4.33 (d, *J* = 6.2 Hz, 2H), 4.17 - 4.04 (m, 4H), 2.97 - 2.73 (m, 4H), 1.85 - 1.58 (m, 5H), 1.51 - 0.24 (m, 74H). ^{13}C NMR (100 MHz, $CDCl_3$) δ 185.71, 185.20, 161.57, 158.03, 157.17, 155.57, 155.44, 155.17, 155.11, 153.37, 153.30, 152.99, 152.85, 152.70, 152.60, 152.49, 152.46, 152.35, 147.10, 146.83, 145.04, 144.84, 137.37, 137.34, 136.51, 136.42, 136.34, 136.02, 134.94, 134.52, 134.29, 133.85, 133.76, 133.47, 132.94, 132.86, 132.63, 130.95, 130.16, 119.64, 119.18, 114.87, 114.67, 114.65, 113.01, 112.88, 112.22, 111.63, 105.00, 100.34, 69.00, 68.67, 55.43, 54.41, 39.19, 31.94, 31.80, 31.45, 30.92, 30.69, 30.44, 29.87, 29.77, 29.65, 29.53, 29.50, 29.38, 29.22, 29.13 25.88, 22.71, 22.56, 22.44, 14.15, 14.05, 14.0. MALDI-MS (m/z) of $C_{93}H_{100}F_4N_8O_4S_5$ for [M^+]: calcd. 1630.17; found, 1630.28.

BTP-POE-D: According to the synthetic process of compound BTP-POE-H, and using Compound 10-D (99 mg, 0.815 mmol) instead of Compound 10, BTP-POE-D was obtained as a blue-black (102 mg, 76.5%). ^{1}H NMR (400 MHz, $CDCl_3$) δ 8.81 (s, 1H), 8.51 (dd, *J* = 9.9, 6.5 Hz, 1H), 8.39 - 8.24 (m, 2H), 7.57 (t, *J* = 7.5 Hz, 1H), 7.42 (t, *J* = 7.5 Hz, 1H), 6.71 (s, 2H), 6.52 (s, 1H), 5.91 (s, 2H), 4.32 (d, *J* = 6.3 Hz, 2H), 2.97 - 2.73 (m, 4H), 1.84 - 1.58 (m, 5H), 1.53 - 0.23 (m, 68H). ^{13}C NMR (100 MHz, $CDCl_3$) δ 185.71, 185.20, 161.59, 158.02, 157.13, 155.57, 155.44, 155.16, 155.09, 153.35, 153.30, 152.98, 152.83, 152.69, 152.57, 152.47, 152.44, 152.33, 147.09, 146.83, 145.03, 144.81, 137.39, 137.31, 136.50, 136.42, 136.34, 136.01, 134.93, 134.51, 134.25, 133.85, 133.75, 133.44, 132.93, 132.85, 132.66, 130.95, 130.18, 119.65, 119.16, 114.86, 114.66, 114.48, 113.01, 112.88, 112.26, 111.62, 105.00,

100.30,69.01, 68.66, 55.44, 54.42, 39.20, 31.94, 31.80, 31.44, 30.93, 30.68, 30.43, 29.86, 29.76, 29.65, 29.52, 29.49, 29.38, 29.21, 29.13, 25.86, 22.71, 22.56, 22.44, 14.15, 14.05, 14.01. MALDI-MS (m/z) of $C_{93}H_{90}D_{10}F_4N_8O_4S_5$ for [M^+]: calcd. 1640.23; found, 1640.37.

2. Fabrication and characterization

OSCs fabrication and measurement:

The conventional device structure of ITO/PEDOT:PSS/active layer/PDINN/Ag was constructed. The indium tin oxide (ITO) substrates (purchased from Liaoning Preferred New Energy Technology Co., Ltd size of 15*15*1 mm, film thickness of 135 nm, sheet resistance 15 Ω sq^{-1}) were prepared in ultrasonic baths in an order of containing detergent, water, deionized water, ethanol, then dried in oven at 80℃ for 10 min. The substrates were treated with ultraviolet ozone for 5 min and the PEDOT: PSS aqueous solution (Baytron P 4083 from H. C. Starck) was filtered through a 0.45 mm filter and then spin-coated on precleaned ITO-coated glass at 6000 rpm for 25 s. After annealing at 150 ℃ on hot plate in the air conditions for 15 min, the substrates were transferred into a N_2 protected glove box. The optimal preparation process of the active layers is that the blend solutions of PM6:SMAs (BTP-POE-H, BTP-POE-D) (1:1.2, w/w, and the total concentration was 18 mg/mL) in chloroform with the addition of a small amount of CN (0.8%, v/v) were spin-coated on PEDOT:PSS films with 4500 RPM in a high purity nitrogen filled glove box. Then the active layers were annealed at 100 °C for 5 min. Detailed device fabrication conditions were

summarized in Table S2-S3. Then, ~10 nm PDINN as cathode interlayer was spin-coated onto the active layers in a concentration of 1 mg/ml in methanol solution. At last, about 100 nm Ag were vacuum thermally deposited on the top of the device through a shadow mask under 10^{-6} Pa vacuum conditions. The device area was exactly fixed at 0.06 cm^2. The current-voltage (J-V) curves of PSCs were measured in a high-purity nitrogen-filled glove box using a Keithley B2901A source meter. AM 1.5G irradiation at 100 mW cm^{-2} is provided by simulator (SS-F5-3A, Enlitech, AAA grade, 70× 70 mm^2 photobeam size) in glove box, which was calibrated by standard silicon solar cells. The external quantum efficiency (EQE) spectra of OSCs were measured in air conditions by a solar cell spectral response measurement system (QE-R3011, Enlitech).

***J-V* and EQE Measurement:** The current density-voltage (*J-V*) characteristics were measured by using the solar simulator (SS-F5-3A, Enlitech, Taiwan) along with AM 1.5G (100 mW/cm^2). The external quantum efficiency (EQE) was recorded with a QE-R measurement system (Enlitech, Taiwan). The effective area of all devices was confined as 0.06 cm^2.

Light-Intensity Dependence Measurements: Light-intensity dependence measurements were performed with PAIOS instrumentation (Fluxim) (steady-state and transient modes). Transient photo-voltage (TPV) measurements monitor the photovoltage decay upon a small optical perturbation during various constant light-intensity biases and at open-circuit bias conditions. Variable light-intensity biases lead to a range of measured V_{OC} values that were used for the analysis. During the

measurements a small optical perturbation (<3% of the V_{OC}, so that $\Delta V_{OC} << V_{OC}$) is applied. The subsequent voltage decay is then recorded to directly monitor bimolecular charge carrier recombination. The photovoltage decay kinetics of all devices follow a mono-exponential decay: $\delta V = A \exp(-t/\tau)$, where t is the time and τ is the charge carrier lifetime. The "charge extraction" (CE) technique was used to measure the charge carrier density n under open-circuit voltage condition. The device is illuminated and kept in open-circuit mode. After light turn-off, the voltage is switched to zero or taken to short-circuit condition to extract the charges. To obtain the number of extracted charges, the current is integrated. The carrier lifetimes follow a power law relationship with charge density: $\tau = \tau_0 n^{-\lambda}$. The bimolecular recombination constants k_{rec} were then inferred from the carrier lifetimes and densities according to $k_{rec} = 1/(\lambda+1)/n\tau^2$, where λ is the recombination order. Photo-CELIV measurements (ramp rate 100 V ms^{-1}, delay time: 0 s, offset voltage: 0 V, light pulse length: 100 μs) were also performed using PAIOS for different light intensities. The light intensity is given in the maximum power of the LED source (100% ≈ 100 mW cm^{-2}).

SCLC mobility measurement (SCLC): The structure of electron-only devices is ITO/ZnO/active layer/PDINN/Ag and the structure of hole-only devices is ITO/PEDOT:PSS/active layer/MoO3/Ag. In these device structures, the same fabrication conditions as OSCs are used to form the active layer films. The charge mobilities are generally described by the Mott-Gurney equation.[1]

$$J = \frac{9}{8}\mu\varepsilon_0\varepsilon_r V^2/L^3$$

where J is the current density, ε_0 is the permittivity of free space (8.85×10^{-14} F cm^{-1}), ε_r is the dielectric constant of used materials, μ is the charge mobility, V is the effective voltage. The effective voltage was obtained by subtracting the built-in voltage (V_{bi}) and the voltage drop (V_s) from the series resistance of the whole device except for the active layers from the applied voltage (V_{appl}), $V = V_{appl} - V_{bi} - V_s$. L is the active layer thickness. The ε_r is assumed to be 3, which is a typical value for organic materials.

In this case, the charge mobilities were estimated using the following equation:

$$\mu = \frac{8}{9}\varepsilon_0\varepsilon_r\left(\frac{\sqrt{J}}{V}\right)^2 L^3$$

^{1}H NMR and ^{13}C NMR: ^{1}H NMR,^{13}C NMR and ^{1}H-^{1}H NOESY NMR spectra were recorded on Bruker AVANCE 400 MHz NMR spectrometer with $CDCl_3$ as a solvent.

MALDI-TOF: MALDI-TOF mass spectrometry experiments were performed on an autoflex III instrument (Bruker Daltonics, Inc.).

TGA: TGA was measured on HTG-1 Thermogravimetric Analyzer (Beijing Hengjiu Experiment Equipment Co. Ltd.) with a heating rate of 10 °C min^{-1} under a nitrogen flow rate of 100 mL min^{-1}.

DSC: DSC measurements were performed on a Mettler Toledo DSC1 star system. The heating rate and cooling rate were both kept 10 ℃ min^{-1} under a nitrogen flow rate of 50 mL min^{-1}. The samples were loaded in aluminum pans directly with another

empty aluminum pan as the reference. As for the blend samples, donor and acceptor materials were solved in chloroform (20 mg ml^{-1} for acceptor, gradient proportion of donor by mass concentration) and stirred overnight. Next, the solvent was spin-coated onto cleaned glass substrates and dried under vacuum to form homogeneous films. The samples were then scraped off the substrates and loaded in aluminum pans.

UV-visible absorption: The UV-vis absorption spectra were measured by Hitachi U-2910 UV-vis spectrophotometer. In the case of solution absorbance measurement, the dilute solution of acceptors in chloroform (1×10^{-5} M) was prepared to be measured. Besides, the thin film samples were prepared by spin-coating (3000 rpm) acceptors' chloroform solutions (10 mg ml^{-1}) on quartz plates. The as-cast thin films all performed a thickness ranging from 50 nm to 80 nm, which were recorded on Bruker DEKTAK XT step profiler.

Cyclic voltammetry: Cyclic voltammetry was conducted on a Zahner IM6e electrochemical workstation using sample films coated on glassy carbon as the working electrode, Pt wire as the counter electrode, and Ag/AgCl as the reference electrode, in a 0.1 M tetrabutylammonium hexafluorophosphate (Bu4NPF6) acetonitrile solution and ferrocene/ferrocenium (Fc/Fc+) couple was used as an internal reference.

AFM: AFM measurements were performed by using Bruker Nano Inc. From America. All film samples were spin-cast on ITO substrates.

TEM: Transmission electron microscope (TEM) studies were conducted with a FEI Tecnai G2 F20 electron microscopy to investigate the phase distribution of the active

layer，and with the scale bar is 200 nm

GIWAXS: The GIWAXS measurements were conducted at the Synchrotron Radiation Facility (SSRF), beamline BL14B1. Part of the GIWAXS data acquisition was also carried out at SSRF beamline BL16B1 and Beiiing Synchrotron Radiation Facility (BSRF) beamline 1W1A. Grazing incidence wide angle scattering (GIWAXS) data were recorded at NCD-SWEET beamline (ALBA synchrotron in Cerdanyola del Vallès, Spain) with a monochromatic (λ = 960299 Å) X-ray beam of 80 × 30 μm^2 [H × V], using a Si (111) channel cut monochromator. The scattered signal was recorded using a Rayonix LX255-HS area detector placed at 241.1 mm from the sample position. The reciprocal q-space and sample-to-detector distance were calculated using LaB_6 as calibrant. A near-critical angle of incidence of 0.13° was used to maximize the thin film signal and the collected 2D patterns were azimuthally integrated using PyFAI.

3 Supplementary Tables

Table S1. GIWAXS structural parameters of the BTP-POE-H, BTP-POE-D, PM6:BTP-POE-H and PM6:BTP-POE-D blend films.

OOP (010)	*q* (Å^{-1})	*d* (Å)	Peak area (Å^2)	*CL* (Å)	
BTP-POE-H	1.67	3.77	3.2	18.1	
BTP-POE-D	1.67	3.76	3.6	20.4	
IP (100)	*q* (Å^{-1})	*d* (Å)	Peak area (Å^2)	*CL* (Å)	
BTP-POE-H	0.32	19.7	1.2	40.8	
BTP-POE-D	0.32	19.7	1.5	41.0	
OOP (100)	*q* (Å^{-1})	*d* (Å)	FWHM (Å^{-1})	*CL* (Å)	Area (×10^7)
PM6:BTP-POE-H	0.30	21.1	0.0796	70.9	7.5
PM6:BTP-POE-D	0.30	21.1	0.0792	71.4	7.7
OOP (010)	*q* (Å^{-1})	*d* (Å)	FWHM (Å^{-1})	*CL* (Å)	Area (×10^7)

PM6:BTP-POE-H	1.71	3.67	0.230	24.7	8.0
PM6:BTP-POE-D	1.72	3.65	0.205	27.6	9.7
IP (100)	q (Å^{-1})	d (Å)	FWHM (Å^{-1})	CL (Å)	Area (×10^7)
PM6:BTP-POE-H	0.30	20.7	0.062	91.3	15.7
PM6:BTP-POE-D	0.31	20.5	0.064	88.1	19.7

Table S2. Photovoltaic performance of the OSCs based on PM6:BTP-POE-H and PM6:BTP-POE-H devices (D/A=1:1.2 (w/w) , total concentration:18 mg/ml, 1% CN, speed: 4000 rpm) with different thermal annealing temperature and time under the illumination of AM 1.5 G at 100 mW cm^{-2}.

Active layer	Thermal annealing	V_{oc} (V)	J_{sc} (mA cm^{-2})	FF (%)	PCE (%)
PM6: BTP-POE-H	80 °C, 5 min	0.874	22.30	75.12	14.63
PM6: BTP-POE-H	80 °C, 10 min	0.874	22.37	74.57	14.60
PM6: BTP-POE-H	100 °C, 5 min	0.878	22.69	75.88	15.11
PM6: BTP-POE-H	100 °C, 10 min	0.875	22.91	75.46	15.13
PM6: BTP-POE-D	80 °C, 5 min	0.873	22.81	75.06	14.95
PM6: BTP-POE-D	80 °C, 10 min	0.877	22.25	75.98	14.82
PM6: BTP-POE-D	100 °C, 5 min	0.881	23.22	77.09	15.77
PM6: BTP-POE-D	100 °C, 10 min	0.876	23.60	74.77	15.45

Table S3. Photovoltaic parameters of the OSCs based on PM6:BTP-POE-H and PM6:BTP-POE-H (D/A=1:1.2 (w/w) , total concentration:18 mg/ml, TA:100 °C/5 min, speed: 4000 rpm) blend with different contents of CN (*v/v*) processed by CF, under the illumination of AM 1.5G, 100 mW cm^{-2}.

Active layer	CN amount (vol)	V_{oc} (V)	J_{sc} (mA cm^{-2})	FF (%)	PCE (%)

PM6: BTP-POE-H	0.5%	0.886	24.04	65.65	13.98
PM6: BTP-POE-H	0.7%	0.882	24.00	76.02	16.09
PM6: BTP-POE-H	0.8%	0.876	24.04	76.54	16.12
PM6: BTP-POE-H	1%	0.870	23.81	76.02	15.74
PM6: BTP-POE-H	1.3%	0.871	23.62	73.53	15.12
PM6: BTP-POE-D	0.5%	0.890	24.79	24.01	14.67
PM6: BTP-POE-D	0.7%	0.886	24.22	23.84	16.40
PM6: BTP-POE-D	0.8%	0.880	24.04	23.66	16.51
PM6: BTP-POE-D	1%	0.880	23.78	23.41	16.26
PM6: BTP-POE-D	1.3%	0.874	23.59	23.22	15.45

4.Supplementary figures

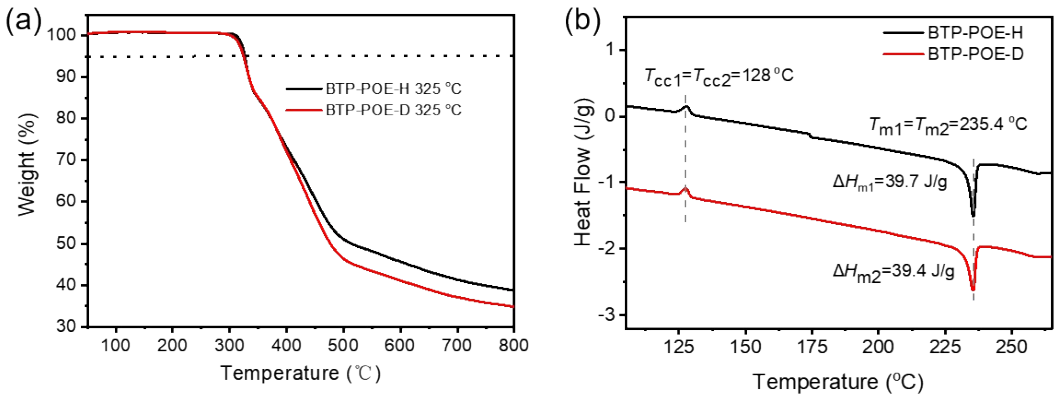

Fig.S1. (a) Thermogravimetric analysis (10 ºC min^{-1}) of BTP-POE-H and BTP-POE-D, respectively. (b) DSC thermograms of the new NFA isomers with a higher heating rate of 10 ºC min^{-1} under nitrogen atmosphere.

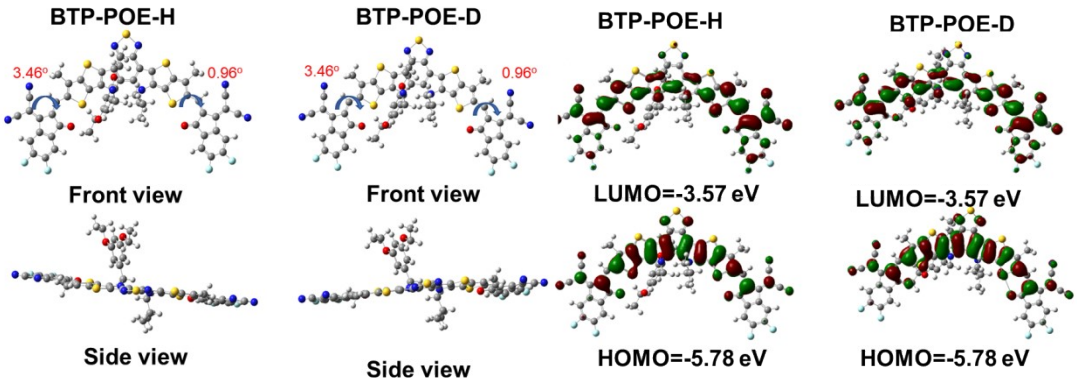

Fig.S2. Optimized geometries, energy levels, and chemical geometry of the molecular models for BTP-POE-H and BTP-POE-D .

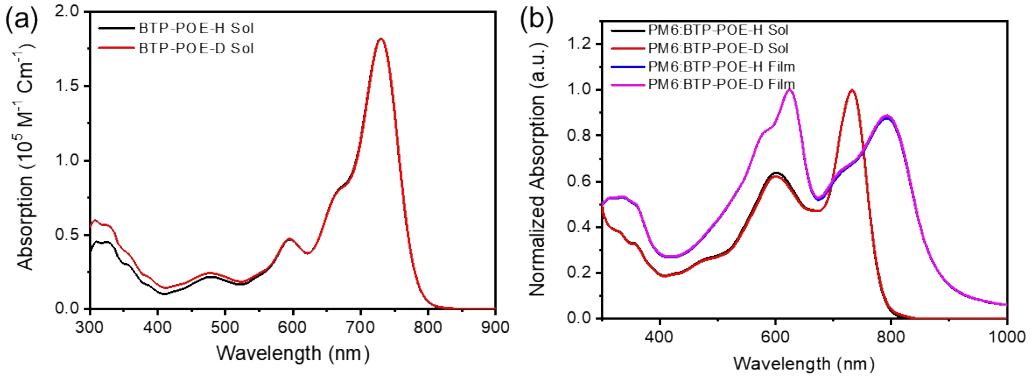

Fig.S3. (a)Absorption spectra of the BTP-POE-H and BTP-POE-D. (b) Absorption spectra of PM6:BTP-POE-H and PM6:BTP-POE-D in chloroform solution and in solid film.

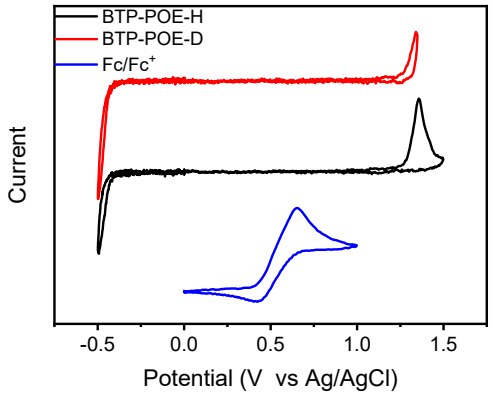

Fig.S4. CV curves of BTP-POE-H and BTP-POE-D.

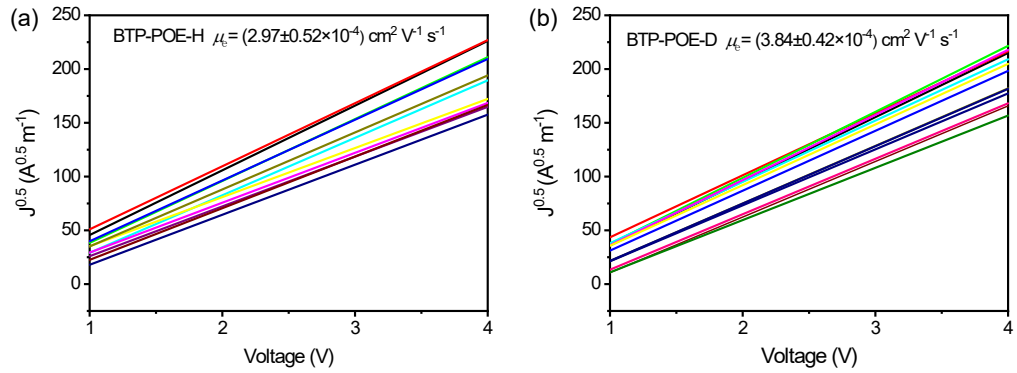

Fig.S5 $J^{1/2}$-V curves of electron-only devices based on the BTP-POE-H and BTP-POE-D films.

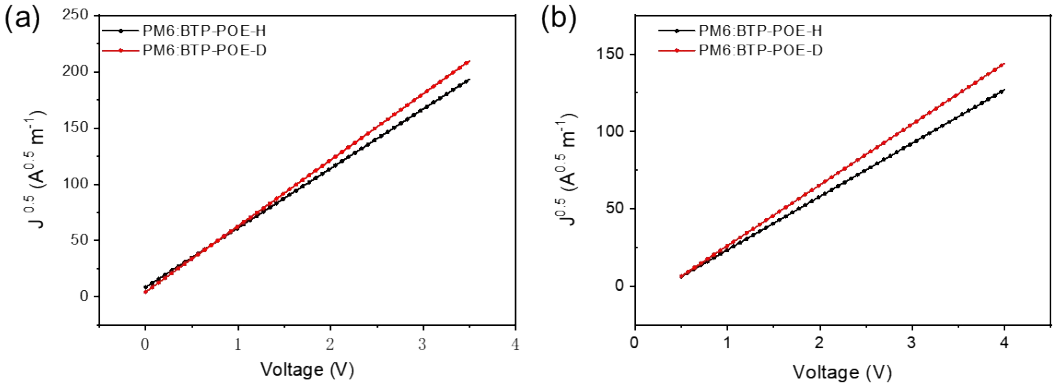

Fig.S6. SCLC fits of hole-only and electron-only devices based on the PM6:BTP-POE-H and PM6:BTP-POE-D blend films

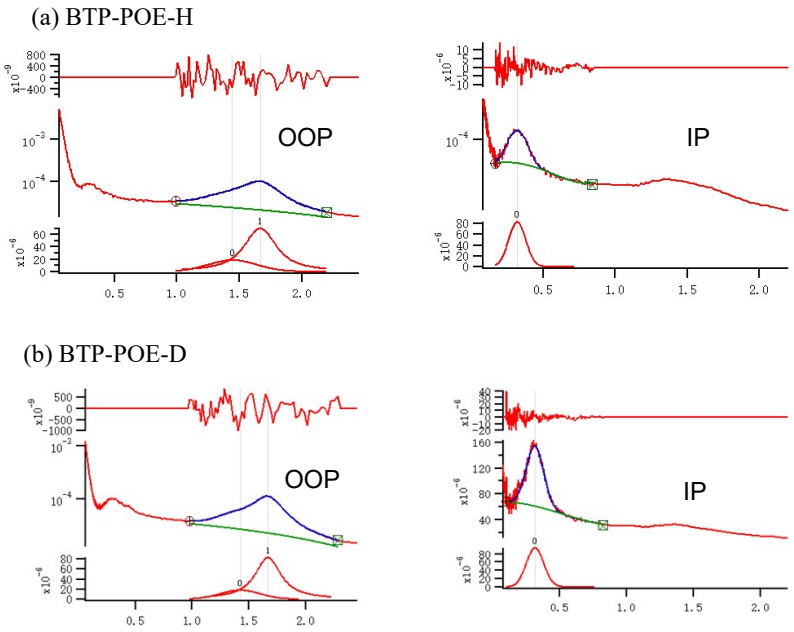

Fig.S7. The multipeak fitting curves of GIWAXS 1D scattering profiles of BTP-POE-H and BTP-POE-D films

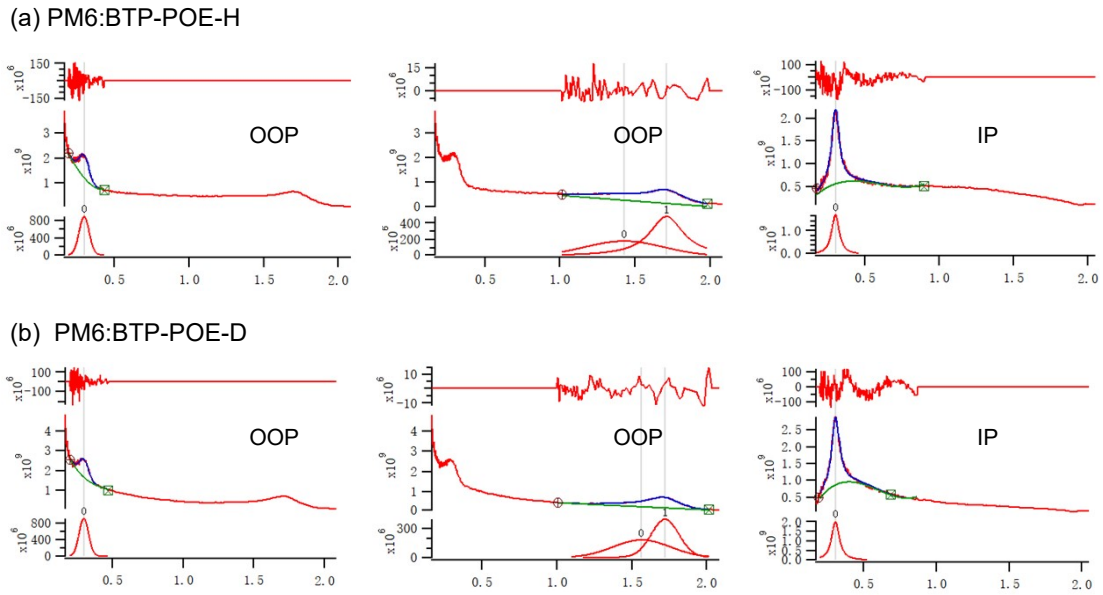

Fig.S8. The multipeak fitting curves of GIWAXS 1D scattering profiles of PM6:BTP-POE-H and PM6:BTP-POE-D blend films

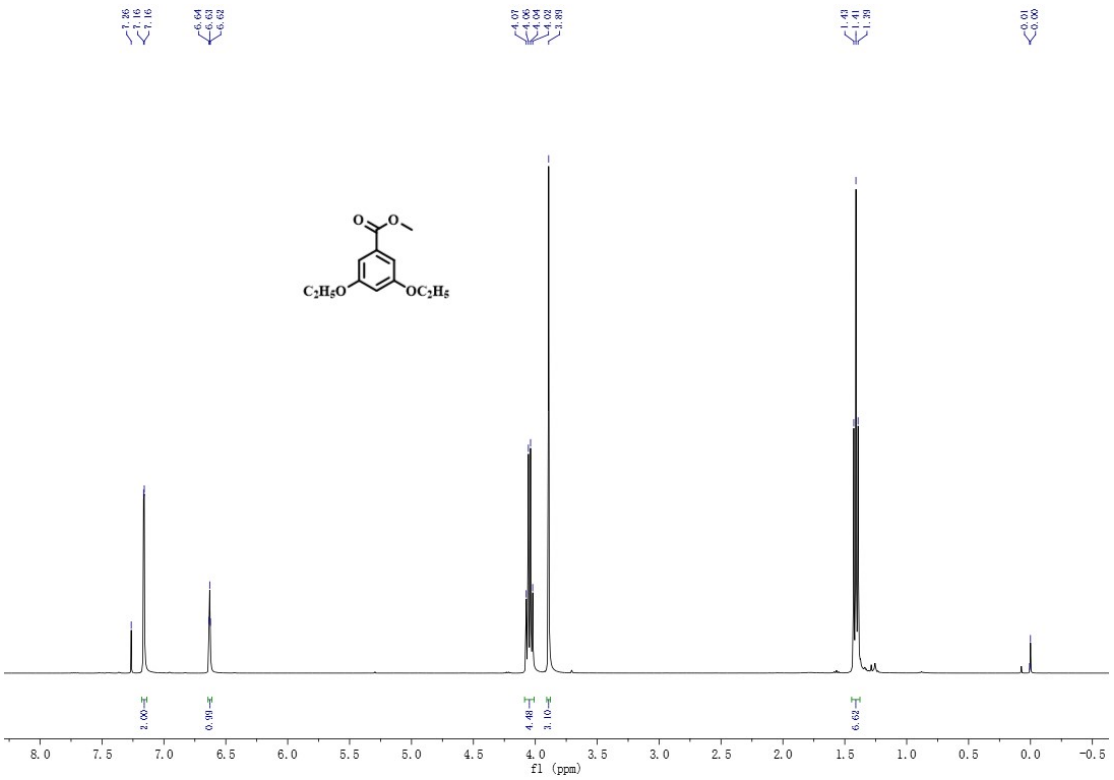

Fig.S9. ^{1}H NMR spectrum of compound 1 ($CDCl_3$).

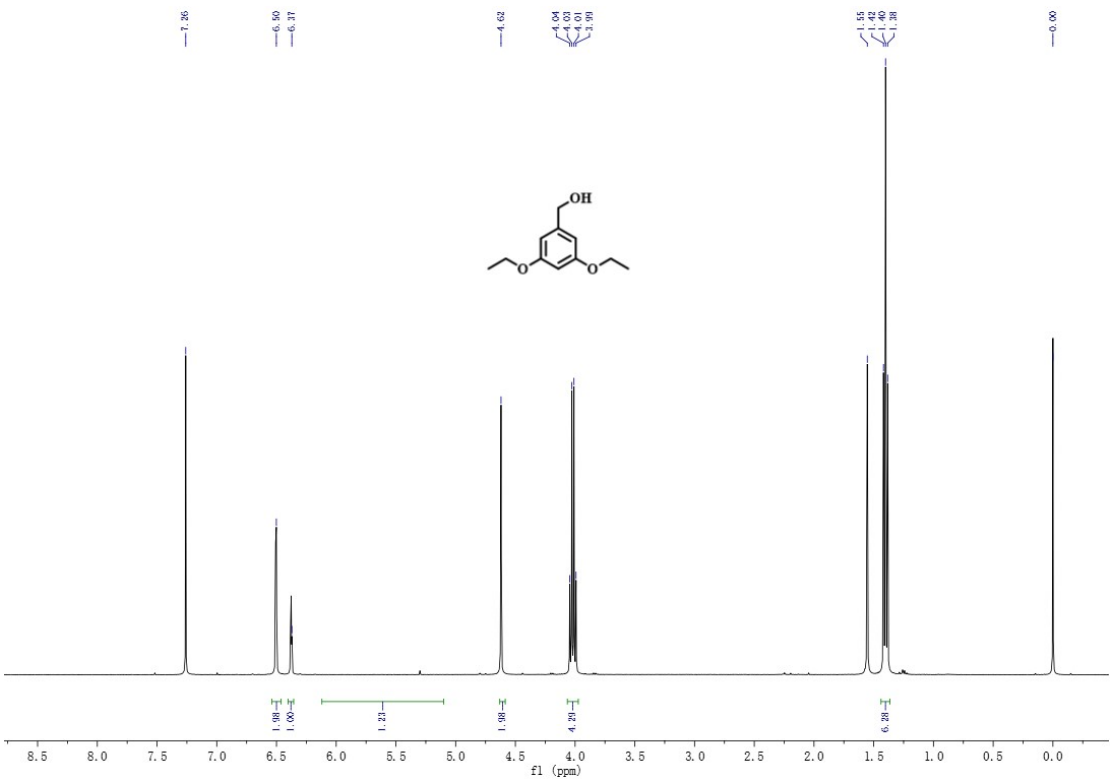

Fig.S10. ^{1}H NMR spectrum of compound 2 ($CDCl_3$).

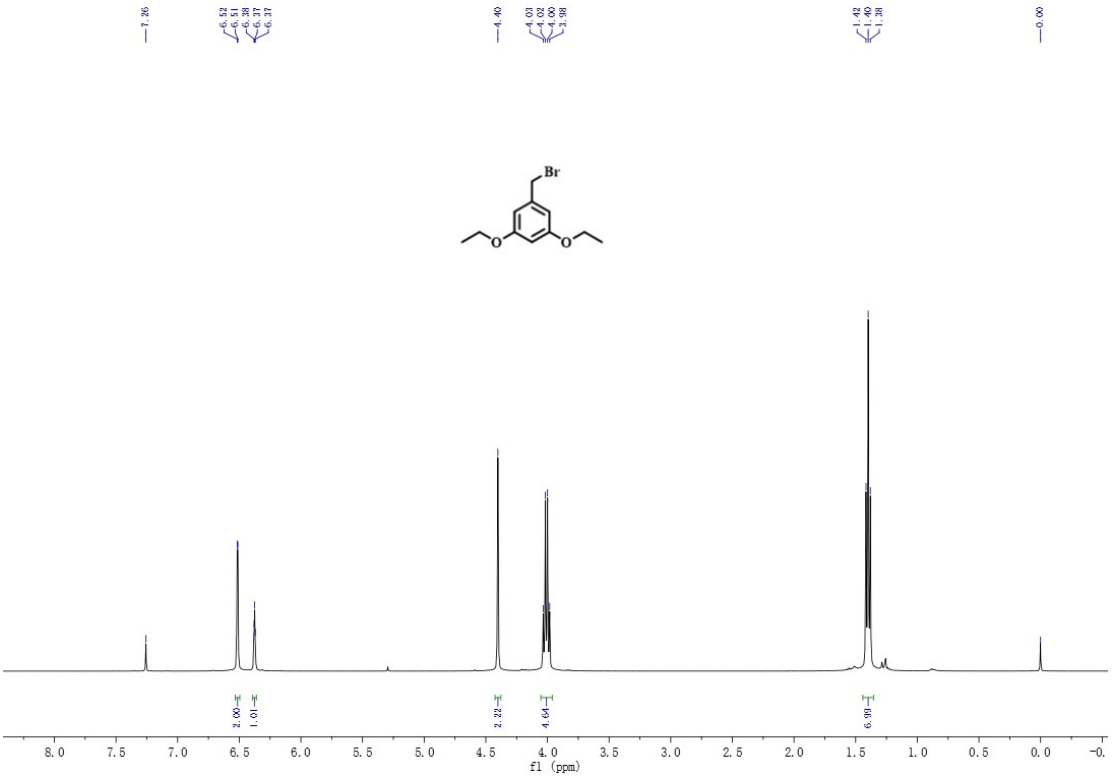

Fig.S11. ^{1}H NMR spectrum of compound 3 ($CDCl_3$).

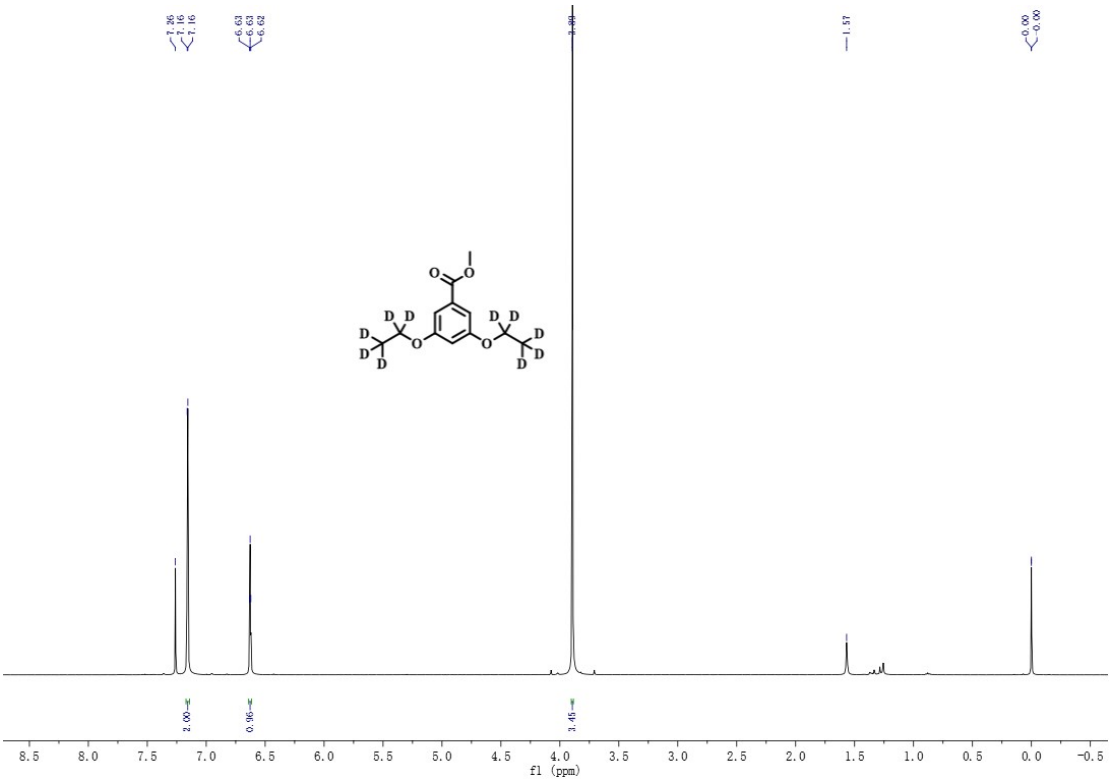

Fig.S12. ^{1}H NMR spectrum of compound 4 ($CDCl_3$).

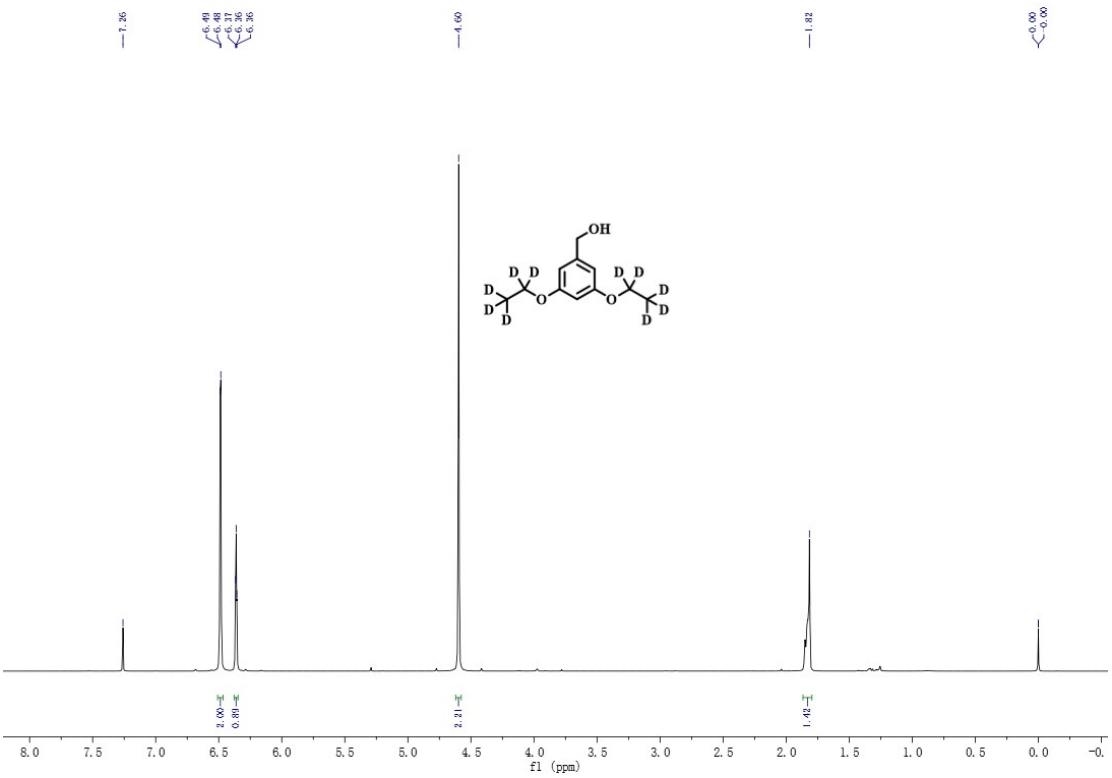

Fig.S13. ^{1}H NMR spectrum of compound 5 ($CDCl_3$).

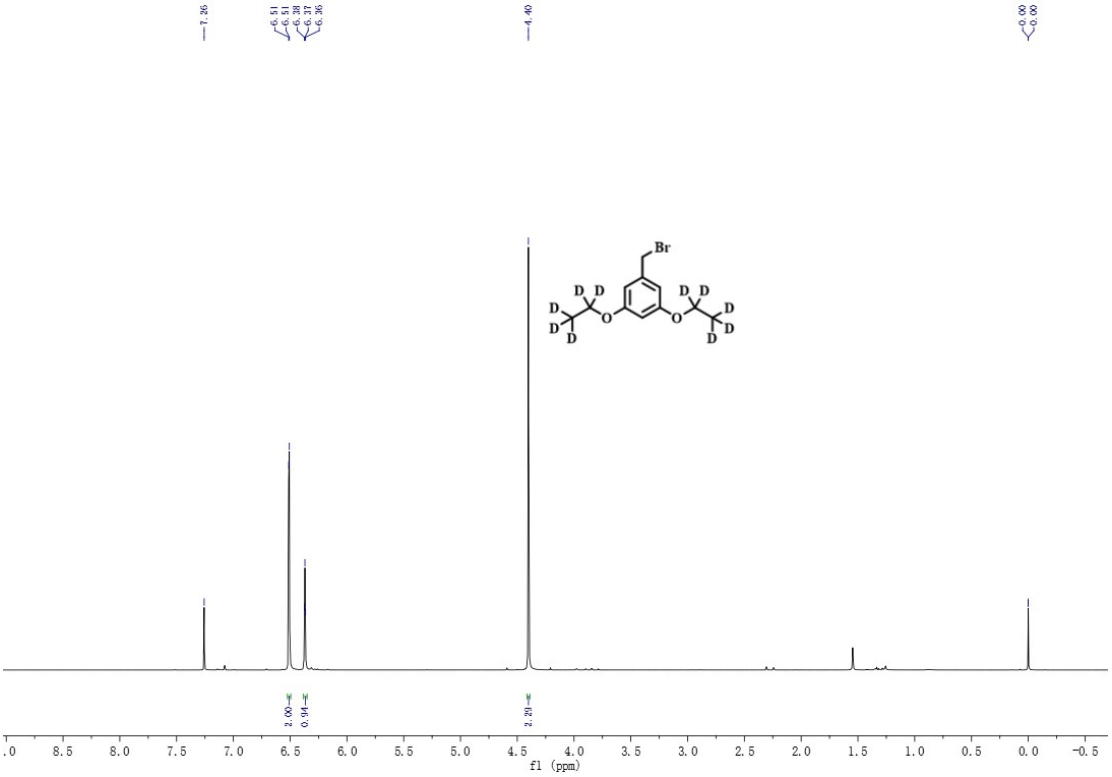

Fig.S14. ^{1}H NMR spectrum of compound 6 ($CDCl_3$).

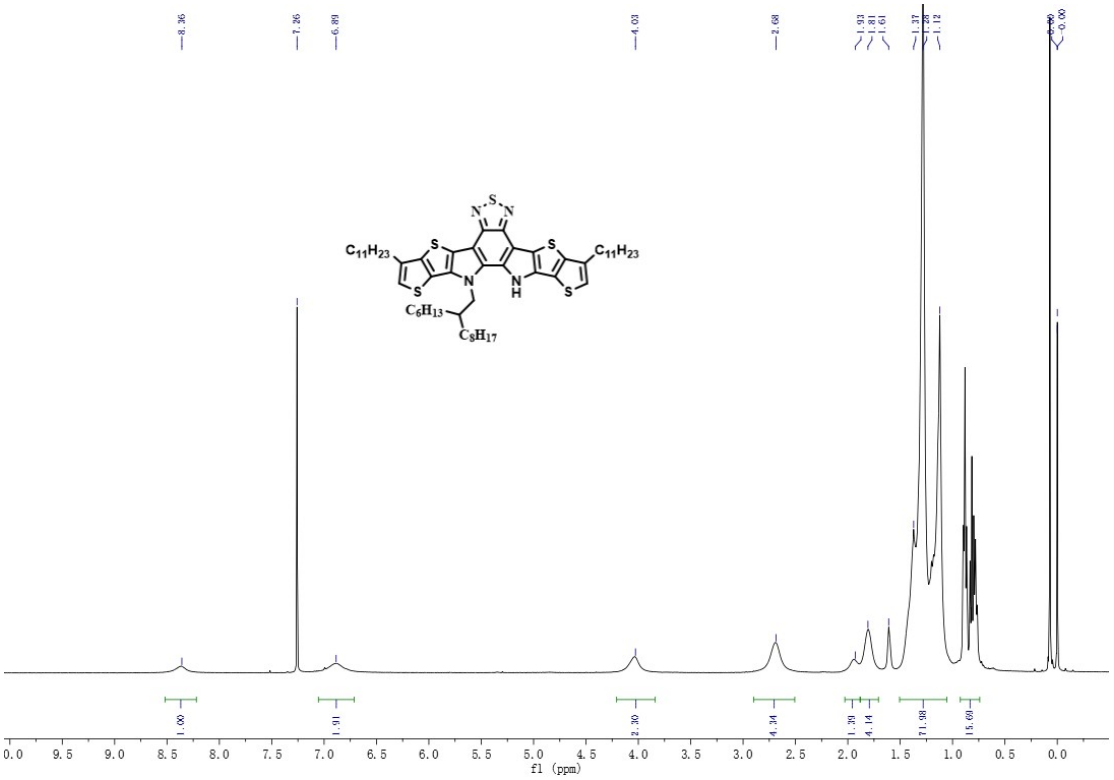

Fig.S15. ^{1}H NMR spectrum of compound 8 ($CDCl_3$).

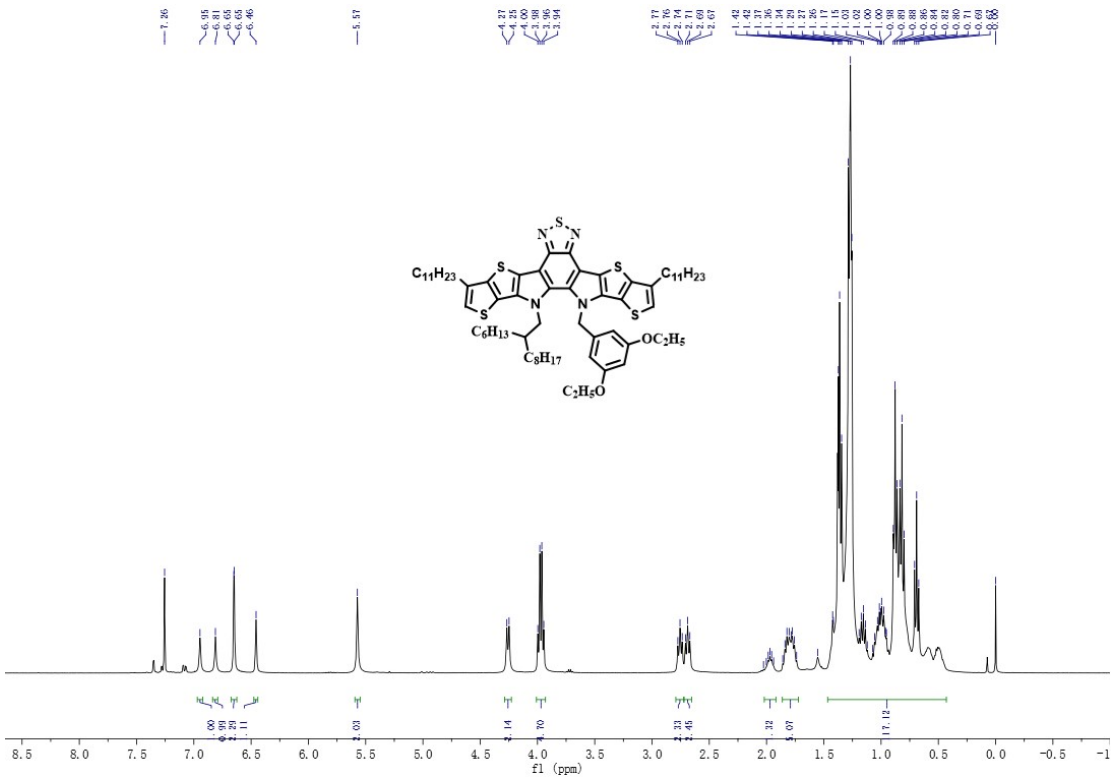

Fig.S16. ^{1}H NMR spectrum of compound 9 ($CDCl_3$).

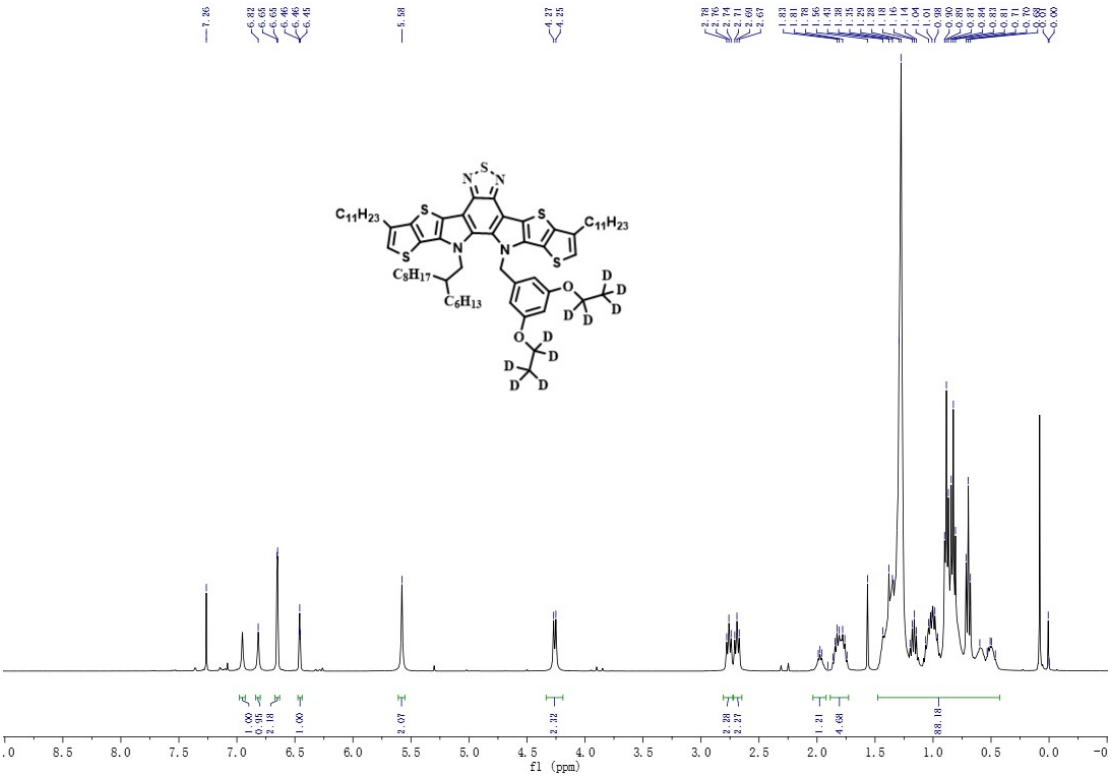

Fig.S17. ^{1}H NMR spectrum of compound 9-D ($CDCl_3$).

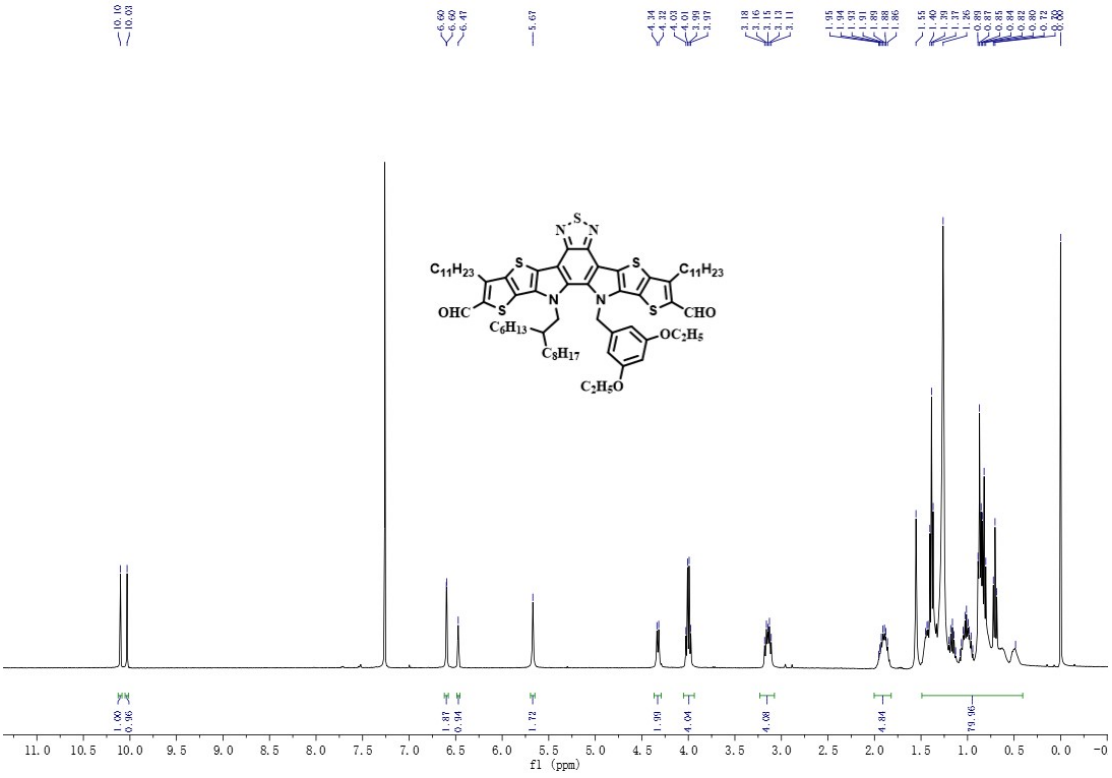

Fig.S18. ^{1}H NMR spectrum of compound 10 ($CDCl_3$).

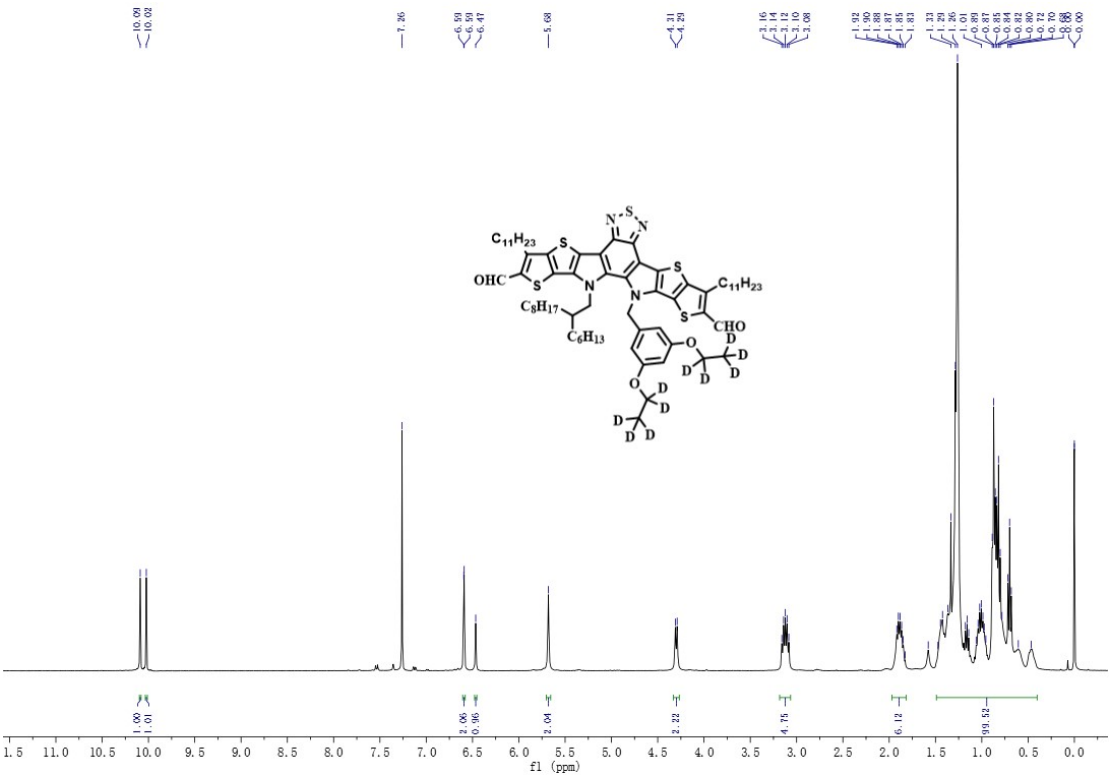

Fig.S19. ^{1}H NMR spectrum of compound 10-D ($CDCl_3$).

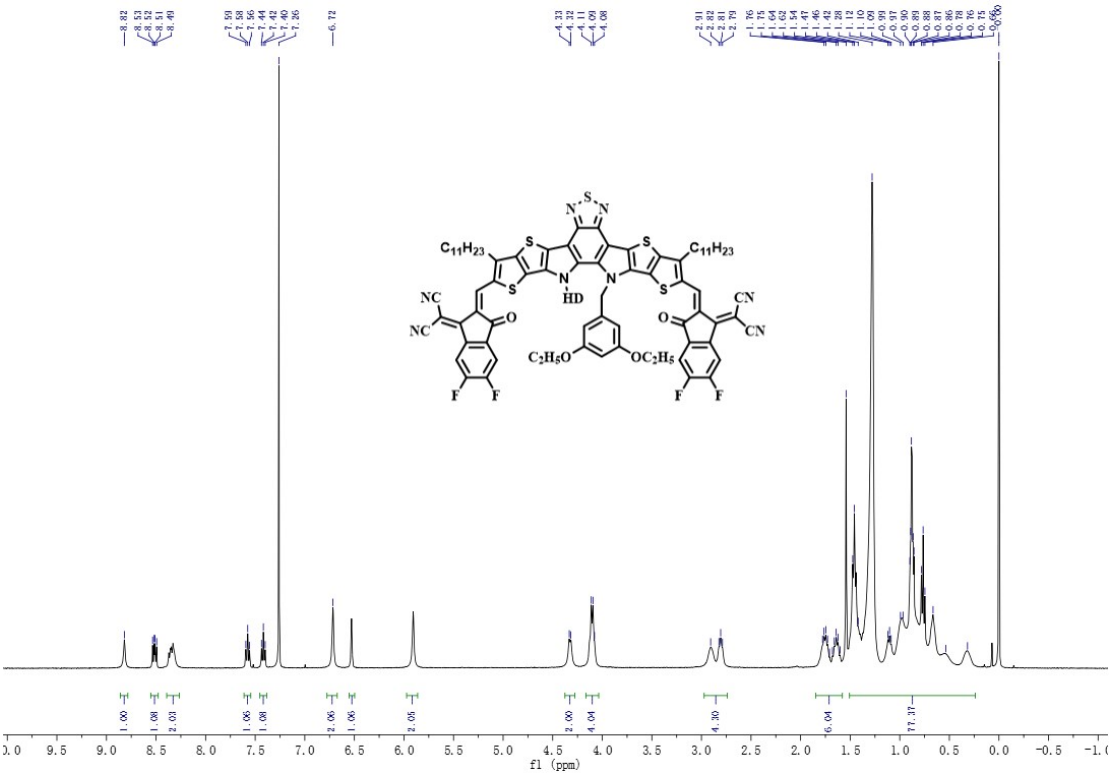

Fig.S20. ^{1}H NMR spectrum of compound BTP-POE-H ($CDCl_3$).

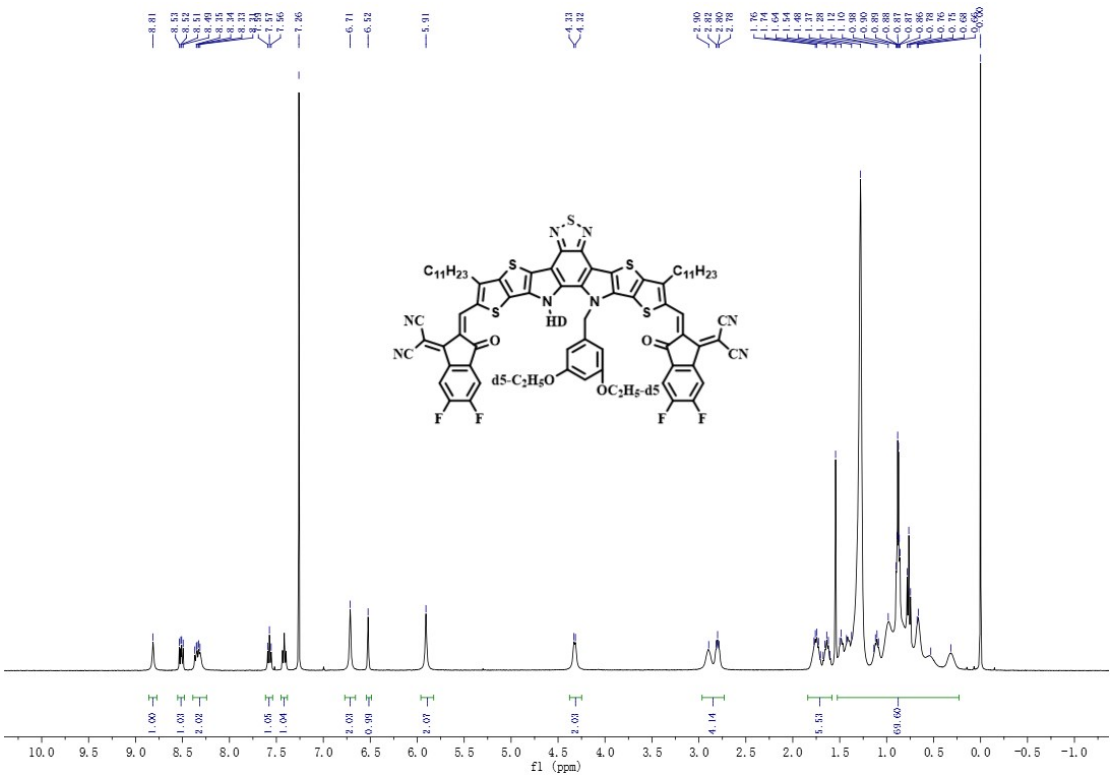

Fig.S21. ^{1}H NMR spectrum of compound BTP-POE-D ($CDCl_3$).

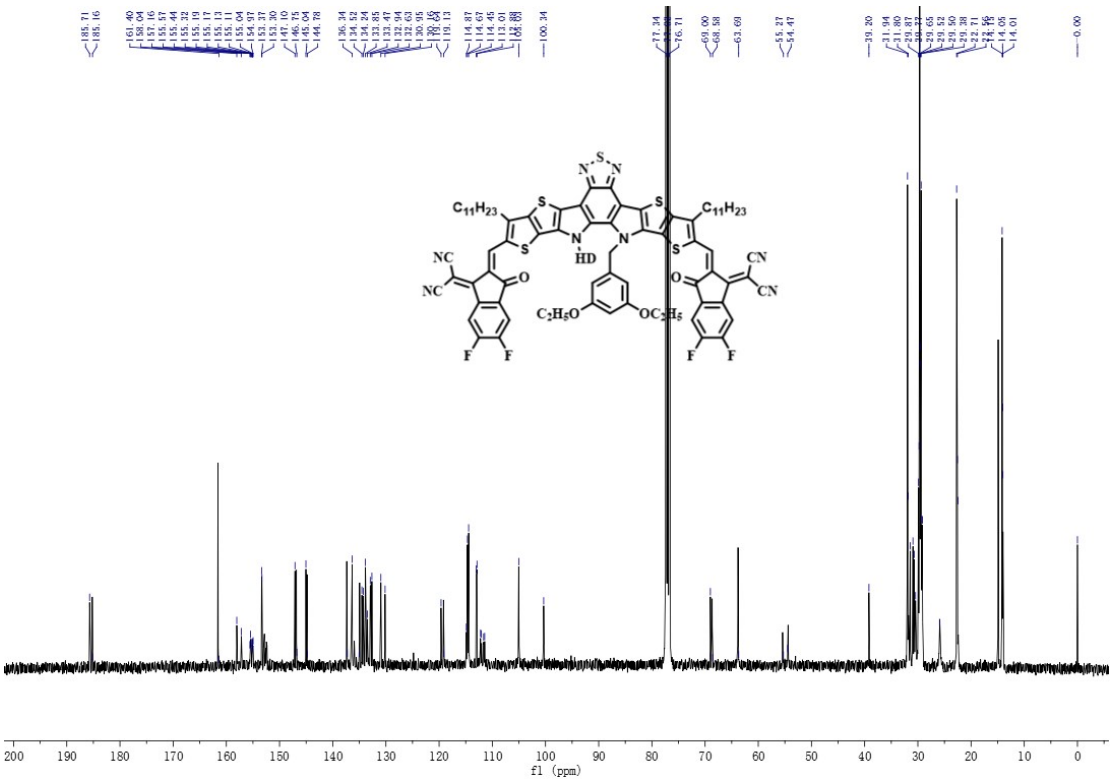

Fig.S22. ^{13}C NMR spectrum of compound BTP-POE-H ($CDCl_3$).

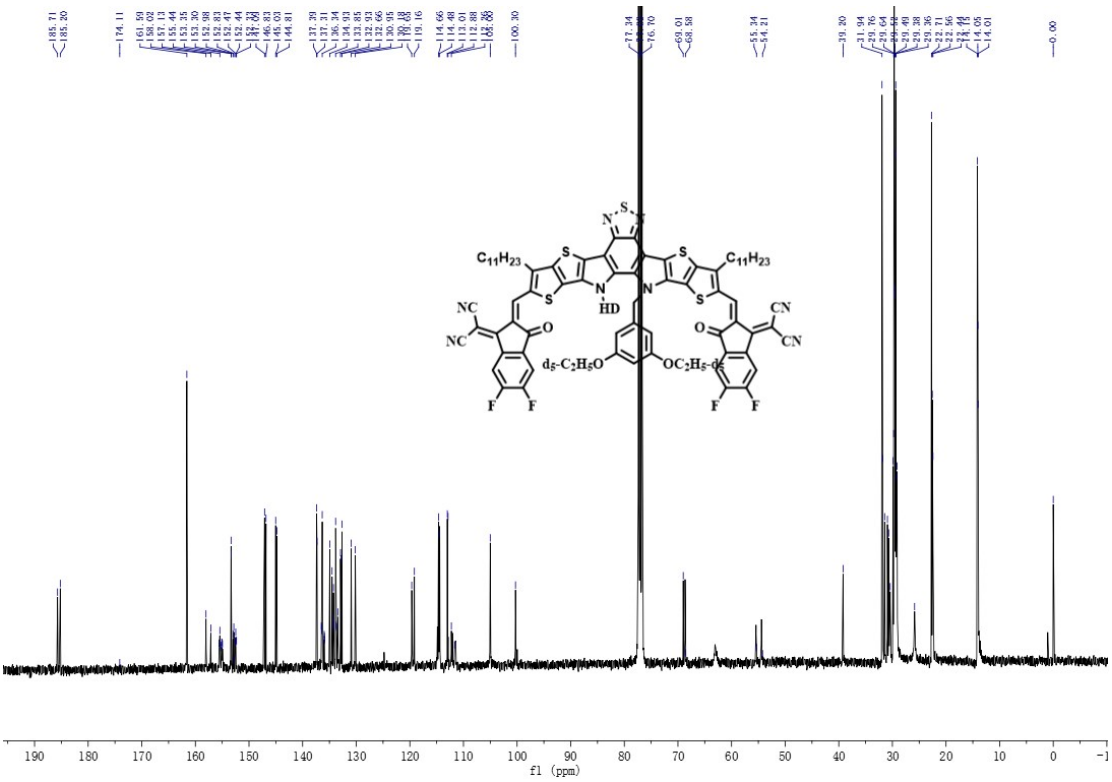

Fig.S23. ^{13}C NMR spectrum of compound BTP-POE-D ($CDCl_3$).

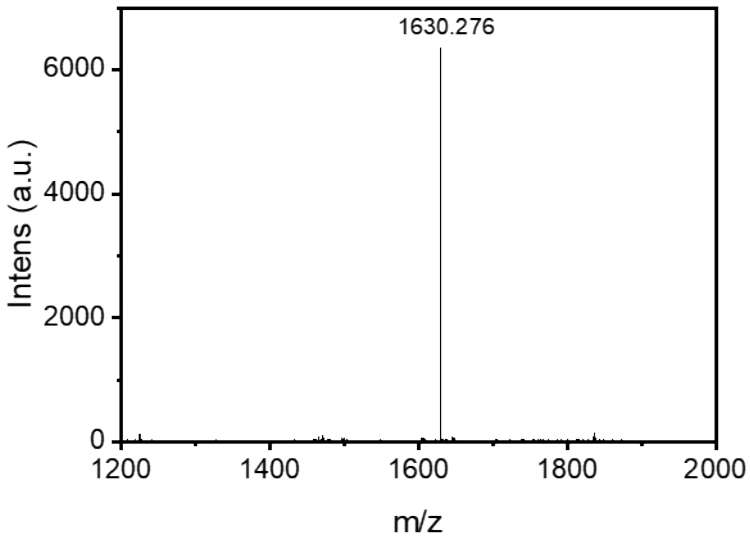

Fig.S24. MALDI-TOF MS spectrum of BTP-POE-H

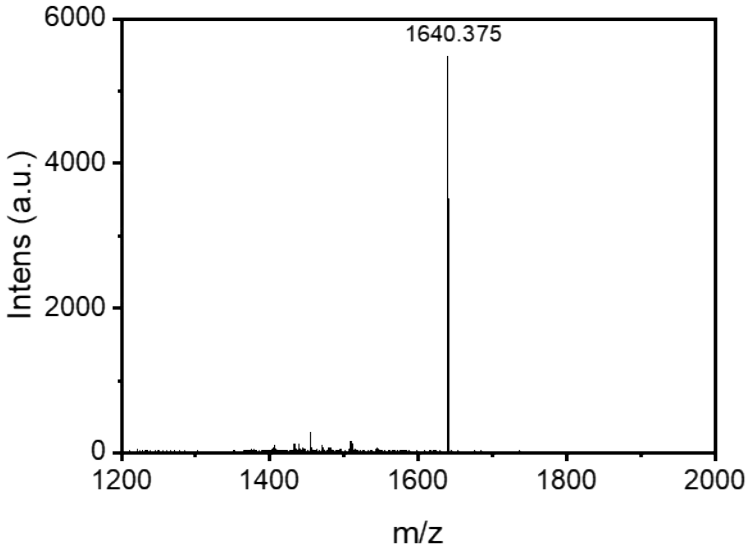

Fig.S25. MALDI-TOF MS spectrum of BTP-POE-D